PUFFIn: Theory

The potential flow solver PUFFIn [1] is presented in this document. After the description of the potential flow equations, the wake generation method and Kutta condition imposed at the trailing edge are presented. Then, the symmetry, anti-symmetry and Neumann-Kelvin conditions are developed from the non-linear free surface condition.

1 General formulation

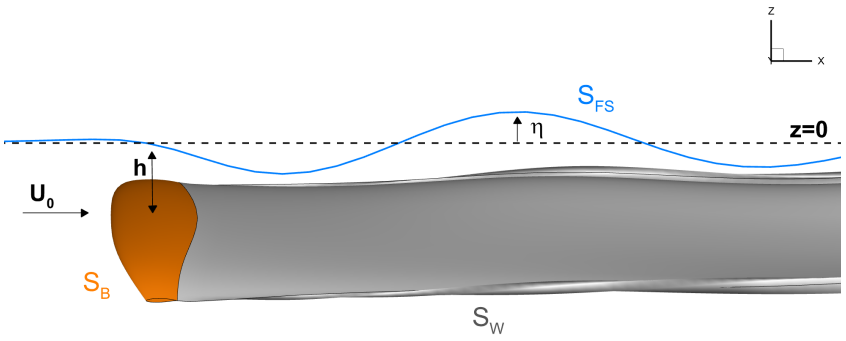

Figure 1: Typical configuration of a lifting surface S_B at low immersion h studied with the potential method.

The solver is based on an incompressible potential approach, i.e. the viscous effects are neglected and the flow is supposed to be irrotational and incompressible. For typical configurations the domain boundary S is the union of the body surface S_B and the free surface boundary S_{FS}. In figure 1, the 3D hydrofoil surface is coloured in orange and only the 2D free surface elevation at mid-span is drawn for the sake of clarity. According to the Kutta-Joukowsky theorem, a circulation has to exist around the surface S_B to generate a lift force. Since the total circulation in the domain should be null, an additional wake surface S_W should exist to counteract the body circulation (Katz et Plotkin [9]). The Kutta condition imposes the wake surface to start at the trailing edge of the hydrofoil, to ensure finite value of the velocity.

The velocity field $\boldsymbol{u}(\boldsymbol{x},t)$ is obtained as the superposition of the undisturbed flow $\boldsymbol{U}_0$ and the gradient of the perturbation potential $\phi(\boldsymbol{x},t)$:

$$\boldsymbol{u}(\boldsymbol{x},t) = \boldsymbol{U}_0 + \boldsymbol{\nabla}\phi(\boldsymbol{x},t) \tag{1}$$

With these assumptions, the mass conservation reduces to a Laplace equation for the velocity perturbation potential:

$$\boldsymbol{\nabla}^2\phi(\boldsymbol{x},t) = 0 \tag{2}$$

Applying the second Green identity to the previous equation, the potential is obtained through a domain Boundary Integral Equation (BIE) written on the domain boundaries S (Hess and Smith [8]):

$$\begin{aligned}
&\phi(\boldsymbol{x},t) = -\frac{1}{4\pi}\int_S \left[\sigma\frac{1}{r} - \mu\frac{\partial}{\partial n}\left(\frac{1}{r}\right)\right] dS \\
&\text{where} \quad r = ||\boldsymbol{x} - \boldsymbol{x_P}||,\ P \in S, \\
&\text{and} \quad \frac{\partial}{\partial n} = \boldsymbol{n}\cdot\boldsymbol{\nabla}, \text{ with } \boldsymbol{n} \text{ the outward pointing normal vector.}
\end{aligned} \tag{3}$$

Equation 3 involves the distributions of doublets μ and sources σ on the boundary S, related with the potential by the relations:

$$\begin{aligned}
\mu(\boldsymbol{x},t) &= -\phi(\boldsymbol{x},t) \\
\sigma(\boldsymbol{x},t) &= -\frac{\partial\phi(\boldsymbol{x},t)}{\partial n}
\end{aligned} \tag{4}$$

The source strengths on the hydrofoil are given by the non-penetration condition, which states that the flow across the surface S_B is zero (Hess and Smith [8]):

$$\sigma(\boldsymbol{x},t) = -\boldsymbol{U}_0\cdot\boldsymbol{n}, \tag{5}$$

The wake should not support any hydrodynamic loads, i.e., the pressure should be continuous at the hydrofoil trailing edge and across the wake surface. Thus, a non-linear Kutta condition (Kutta [10]) is imposed at the trailing edge to obtain the equality of the pressure on the pressure side and suction side of the hydrofoil:

$$p_{\mathrm{TE}}^{\mathrm{PS}} = p_{\mathrm{TE}}^{\mathrm{SS}} \tag{6}$$

where $p_{\mathrm{TE}}^{\mathrm{PS}}$ is the pressure on the pressure side et $p_{\mathrm{TE}}^{\mathrm{SS}}$ the pressure on the suction side. With the Bernoulli relation, the previous equation might be written:

$$p_{\mathrm{TE}}^{\mathrm{PS}} - p_{\mathrm{TE}}^{\mathrm{SS}} = \left[\rho\frac{\partial\phi}{\partial t} + \frac{1}{2}\rho(\boldsymbol{U}_0 + \nabla\phi)^2 + gz\right]_{\mathrm{PS}}^{\mathrm{SS}} \tag{7}$$

where $[a]_{\mathrm{PS}}^{\mathrm{SS}}$ is the difference between the pressure side and suction side values of the quantity a.

To ensure that the wake does not support any pressure jump, the sources distribution on S_W must be null and equation 3 can be written (Katz et Plotkin [9]):

$$\phi(\boldsymbol{x},t) = -\frac{1}{4\pi}\int_{S_B+S_{FS}} \left[\sigma(\boldsymbol{x},t)\frac{1}{r} - \mu(\boldsymbol{x},t)\frac{\partial}{\partial n}\left(\frac{1}{r}\right)\right] dS + \frac{1}{4\pi}\int_{S_W}\left[\mu(\boldsymbol{x},t)\frac{\partial}{\partial n}\left(\frac{1}{r}\right)\right] dS \tag{8}$$

In addition, a kinematic condition is imposed on the free surface :

$$\frac{\partial\eta(\boldsymbol{x},t)}{\partial t} + (\boldsymbol{U}_0 + \boldsymbol{\nabla}\phi(\boldsymbol{x},t))\cdot\boldsymbol{\nabla}\eta(\boldsymbol{x},t) = \frac{\partial\phi(\boldsymbol{x},t)}{\partial z} \quad \text{for} \quad z = \eta \tag{9}$$

where $\eta(x,y)$ is the elevation of the free surface. A dynamic condition is also obtained on the free surface with the Bernoulli relation:

$$\frac{\partial\phi(\boldsymbol{x},t)}{\partial t} + \boldsymbol{U}_0\cdot\boldsymbol{\nabla}\phi(\boldsymbol{x},t) + \frac{1}{2}(\boldsymbol{\nabla}\phi(\boldsymbol{x},t))^2 + g\eta = 0 \quad \text{for} \quad z = \eta \tag{10}$$

These two conditions are non-linear since both relations contain quadratic terms and are written on the deformed free surface ($z = \eta$), which is unknown *a priori*. In order to reduce the computation time, linearised conditions are used, as discussed in section 2.

2 Linearised free surface conditions

For the non-linear free surface conditions, the kinematic and dynamic conditions should be imposed on the deformed interface. To reduce the computational time, the non-linear free surface conditions can be linearised around the initial free surface position $z = 0$. Keeping only the first order terms, the linearised conditions are:

$$\begin{aligned} \frac{\partial \eta}{\partial t} + \boldsymbol{U}_0 \cdot \boldsymbol{\nabla} \eta &= \frac{\partial \phi}{\partial z} \quad \text{in} \quad z = 0 \\ \frac{\partial \phi}{\partial t} + \boldsymbol{U}_0 \cdot \boldsymbol{\nabla} \phi &= -g\eta \quad \text{in} \quad z = 0 \end{aligned} \tag{11}$$

Combining these two equations, the linear Neumann-Kelvin (NK) formulation is obtained (Brard [3]):

$$\left(\frac{\partial}{\partial t} + \boldsymbol{U_0} \cdot \boldsymbol{\nabla} \right)^2 \phi + g \frac{\partial \phi}{\partial z} = 0 \tag{12}$$

Once the velocity potential is known from equation (12), the free surface elevation η can be obtained from the linear kinematic condition (equation (11)).

The asymptotic analysis of the NK formulation allows to further simplify the free surface condition for very small Froude numbers (Fr$<<$ 1) and very large Froude numbers (Fr$>>$ 1). With a characteristic length of the problem L, a non-dimensional equation might be written for 1-dimensional steady problems (Newman [12]):

$$\frac{\partial^2 \phi}{\partial \tilde{x}^2} + \frac{1}{\mathrm{Fr}^2} \frac{\partial \phi}{\partial \tilde{z}} = 0 \quad \text{with} \quad \tilde{x} = \frac{x}{L} \quad \text{and} \quad \tilde{z} = \frac{z}{L} \tag{13}$$

With this formulation, the asymptotic behaviour of the NK condition with the Froude number is transparent:

- For Fr$\to$ 0, equation (13) reduces to $\quad \frac{\partial \phi}{\partial \tilde{z}} \approx 0$ at $\tilde{z} = 0$
- For Fr$\to \infty$, equation (13) reduces to $\quad \frac{\partial^2 \phi}{\partial \tilde{x}^2} \approx 0 \to \phi = 0$ at $\tilde{z} = 0$

For low Froude numbers, the free surface condition can therefore be replaced by a symmetry condition at $z = 0$, while an anti-symmetry condition (also called biplane approximation) may be used for large Froude numbers (Faltinsen [5]). One advantage of the symmetry and anti-symmetry conditions is that the free surface does not need to be meshed, reducing the computational time and potential numerical errors. Typical Froude numbers for the flow around a hydrofoil are relatively high, such as Fr > 3. The symmetry and anti-symmetry conditions are simply obtained by placing a mirrored foil above the free surface with the same or opposite distributions of sources and doublets in the computations.

3 Discretisation and resolution

To construct a numerical solution, the boundaries S_B, S_{FS} and S_W are discretised using quadrilateral elements. The sources and doublets are supposed to be constant on each element. This choice to use low-order distributions instead of higher order methods is dictated by the need to get a fast solver for the multi-fidelity framework. The NK condition is solved using the finite difference method, with the second order upwind scheme proposed by Dawson [4] (see also Bal and Kinnas [2]) for the spatial derivative. At the upstream boundary of the free surface, the first and second derivative of the potential in the stream-wise direction are imposed to be null (Nakos and Sclavounos [11]).

The position of the wake surface is an unknown of the problem. The surface S_W could be to prescribed such that the wake leaves the trailing edge at the median trailing angle or that the wake panels are parallel to the undisturbed flow U_0. However, for the two-body configuration, the wake of the front wing can have a strong influence on the incoming flow experienced by the stabilizer. Thus, a more sophisticated wake model is needed. Since the wake should not support any hydrodynamic loads, the

Kutta-Joukowski theorem imposes that the wake panels are parallels to the local velocity $\boldsymbol{u}(\boldsymbol{x}, t)$ (Katz et Plotkin [9]). This condition is ensured using a Lagrangian time-marching approach for the construction of the wake surface. At each time step, a new set of panels are shed from the hydrofoil trailing edge and the strength of the doublet μ_w on these panels is obtained with the Kutta condition (equation (7)). The new wake panels are obtained by convecting the trailing edge nodes during one time step, so the size of the wake panels depend on the time step value (figure 2). Once a new panel is shed at the time step n, it is convected by the local flow downstream the hydrofoil at the following time steps $m > n$. According to the Kelvin's circulation theorem, the strength of a wake doublet should not change with time. Thus, once a wake panel is generated at the trailing edge, the value of the doublet μ_w is kept constant while it is convected downstream. Because panels far from the hydrofoil have a small contribution to the flow around the hydrofoil, this time marching method allows to obtain the steady state solution. For some two-body configuration, the wake panels might impinge the stabilizer, leading to numerical instabilities. To avoid such problems, several viscous vortex core models are implemented in PUFFIn following the method proposed by Gennaretti and Bernardini [7].

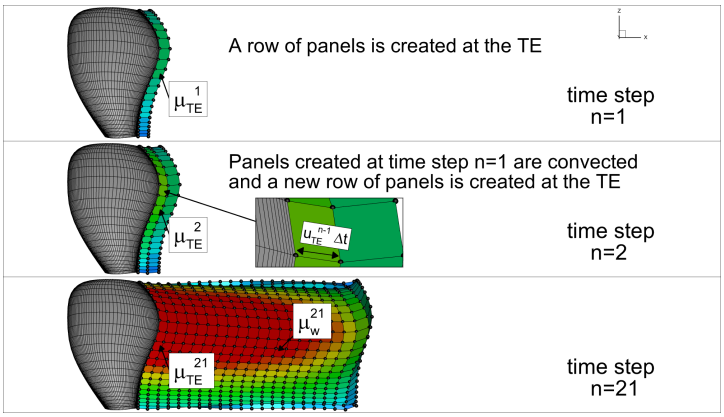

Figure 2: Generation of the wake panels.

While higher order schemes are necessary for true unsteady problems (Filippas et Belibassakis [6]), a first order scheme in time is sufficient to obtain an accurate steady solution with the time-marching algorithm. At time step n, the discretisation of equation (8) at the geometrical centre of each element gives:

$$\begin{bmatrix} \boldsymbol{\mathcal{A}_B} & \boldsymbol{\mathcal{A}_{FS}} \end{bmatrix} \begin{bmatrix} \boldsymbol{\mu_B^n} \\ \boldsymbol{\mu_{FS}^n} \end{bmatrix} = \begin{bmatrix} \boldsymbol{\mathcal{B}_B} & \boldsymbol{\mathcal{B}_{FS}} \end{bmatrix} \begin{bmatrix} \boldsymbol{\sigma_B} \\ \boldsymbol{\sigma_{FS}^n} \end{bmatrix} + \begin{bmatrix} \boldsymbol{\mathcal{W}}^n & \boldsymbol{\mathcal{T}}^n \end{bmatrix} \begin{bmatrix} \boldsymbol{\mu_W^n} \\ \boldsymbol{\mu_{TE}^n} \end{bmatrix} \tag{14}$$

where $\boldsymbol{\mathcal{A}_B}$, $\boldsymbol{\mathcal{A}_{FS}}$, $\boldsymbol{\mathcal{B}_B}$ and $\boldsymbol{\mathcal{B}_{FS}}$ are the matrices containing the influence coefficients for the hydrofoil and the free surface boundaries. The vectors $\boldsymbol{\mu_B^n}$, $\boldsymbol{\mu_{FS}^n}$, $\boldsymbol{\sigma_B^n}$ and $\boldsymbol{\sigma_{FS}^n}$ contain the values of the doublet and the sources at the time step n on the hydrofoil and free surface panels, respectively. The wake panels are split between the first row of panels at the trailing edge and the rest of the wake panels. Indeed, at each time step, the values of the doublets on the first row of panels $\boldsymbol{\mu_{TE}^n}$ are unknown, whereas the doublets on the rest of the wake panels $\boldsymbol{\mu_W^n}$ are known from previous time steps. The matrices $\boldsymbol{\mathcal{T}}^n$ and $\boldsymbol{\mathcal{W}}^n$ contain the influence coefficients of the wake panels. Because the positions of the wake panels change at each time step, these two matrices are therefore time-dependent.

The discretised Neumann-Kelvin equation (12) can be written:

$$\boldsymbol{\mathcal{N}} \boldsymbol{\mu_{FS}^n} = \boldsymbol{\sigma_{FS}^n} + \boldsymbol{\mathcal{Q}} \boldsymbol{\mu_{FS}^{n-1}} \tag{15}$$

where the matrix $\boldsymbol{\mathcal{N}}$ and $\boldsymbol{\mathcal{P}}$ contain the coefficients of the finite difference method.

The Kutta condition is also discretised using the finite difference method, with a second order scheme for the spatial derivative. The discretised Kutta condition can be written:

$$\boldsymbol{\mathcal{M}} \boldsymbol{\mu_B^n} = \boldsymbol{\mathcal{K}} \left(\boldsymbol{\mu_B^n} \right) \boldsymbol{\mu_B^n} + \boldsymbol{\mathcal{P}} \boldsymbol{\mu_B^{n-1}} \tag{16}$$

with $\boldsymbol{\mathcal{M}}$, $\boldsymbol{\mathcal{K}}(\boldsymbol{\mu}_{\boldsymbol{B}}^n)$ and $\boldsymbol{\mathcal{P}}$ the matrices containing the coefficients of the finite difference method. Note that, since the Kutta condition is non-linear, the matrix $\boldsymbol{\mathcal{K}}$ depends on the current value of the doublets $\boldsymbol{\mu}_{\boldsymbol{B}}^n$. Combining equations (14), (15) and (16), the unknown doublet distribution can be obtained by solving:

$$\begin{bmatrix} \mathbf{0} & \tilde{\boldsymbol{\mathcal{M}}} \\ -\boldsymbol{\mathcal{T}}^n & \boldsymbol{\mathcal{A}} \end{bmatrix} \begin{bmatrix} \boldsymbol{\mu}_{\boldsymbol{TE}}^n \\ \boldsymbol{\mu}^n \end{bmatrix} = \begin{bmatrix} \boldsymbol{\mathcal{K}}\left(\boldsymbol{\mu}_{\boldsymbol{B}}^n\right) \boldsymbol{\mu}_{\boldsymbol{B}}^n \\ \boldsymbol{\mathcal{B}}_{\boldsymbol{B}} \boldsymbol{\sigma}_{\boldsymbol{B}} + \boldsymbol{\mathcal{W}}^n \boldsymbol{\mu}_{\boldsymbol{W}}^n \end{bmatrix} + \boldsymbol{\mathcal{R}} \boldsymbol{\mu}^{n-1}$$
$$\text{with} \quad \boldsymbol{\mathcal{A}} = \begin{bmatrix} \boldsymbol{\mathcal{A}}_{\boldsymbol{B}} & \boldsymbol{\mathcal{A}}_{\boldsymbol{FS}} - \boldsymbol{\mathcal{B}}_{\boldsymbol{FS}} \boldsymbol{\mathcal{N}} \end{bmatrix}, \quad \boldsymbol{\mu} = \begin{bmatrix} \boldsymbol{\mu}_{\boldsymbol{B}} \\ \boldsymbol{\mu}_{\boldsymbol{FS}} \end{bmatrix} \quad \text{and} \quad \tilde{\boldsymbol{\mathcal{M}}} = \begin{bmatrix} \boldsymbol{\mathcal{M}} \\ \mathbf{0} \end{bmatrix} \tag{17}$$

A bloc inversion is used to solve Equation (17). The inverse of the Schur complement $\boldsymbol{\mathcal{C}}^{-1} = \left(\boldsymbol{\mathcal{M}} \boldsymbol{\mathcal{D}}^{-1} \boldsymbol{\mathcal{T}}^n\right)^{-1}$ needs to be computed at each time step, since the matrix $\boldsymbol{\mathcal{T}}^n$ is time-dependant. Nevertheless, the matrix inversion does not require a large computational time because the size of the square matrix $\boldsymbol{\mathcal{C}}$ is only the number of panels on the trailing edge square. The inverse matrix $\boldsymbol{\mathcal{A}}^{-1}$ can be computed only once at the beginning of the simulation with a lower-upper (LU) decomposition. An iterative procedure is used at each time step: the non-linear term $\boldsymbol{\mathcal{K}}\left(\boldsymbol{\mu}_{\boldsymbol{B}}^n\right) \boldsymbol{\mu}_{\boldsymbol{B}}^n$ is computed using the value of $\boldsymbol{\mu}_{\boldsymbol{B}}^n$ at the previous iteration.

Once the velocity potential is known, the pressure distribution on the hydrofoil is obtained with the Bernoulli relation. Integration of the pressure over the surface S_B gives the hydrodynamic pressure forces and moments acting on the hydrofoil.

References

[1] Puffin documentation. `https://www.ensta-bretagne.fr/fr/optifoil`, 2023.

[2] S Bal and SA Kinnas. A bem for the prediction of free surface effects on cavitating hydrofoils. *Computational Mechanics*, 28(3):260–274, 2002.

[3] R Brard. The representation of a given ship form by singularity distributions when the boundary condition on the free surface is linearized. *Journal of Ship Research*, 16(01):79–92, 1972.

[4] CW Dawson. A practical computer method for solving ship-wave problems. In *Proceedings of Second International Conference on Numerical Ship Hydrodynamics*, pages 30–38, 1977.

[5] OM Faltinsen. *Hydrodynamics of high-speed marine vehicles*. Cambridge university press, 2005.

[6] ES Filippas and KA Belibassakis. Hydrodynamic analysis of flapping-foil thrusters operating beneath the free surface and in waves. *Engineering Analysis with Boundary Elements*, 41:47–59, 2014.

[7] M Gennaretti and G Bernardini. Novel boundary integral formulation for blade-vortex interaction aerodynamics of helicopter rotors. *AIAA journal*, 45(6):1169–1176, 2007.

[8] JL Hess and AMO Smith. Calculation of nonlifting potential flow about arbitrary three-dimensional bodies. *Journal of ship research*, 8(04):22–44, 1964.

[9] J Katz and A Plotkin. *Low-speed aerodynamics*, volume 13. Cambridge university press, 2001.

[10] WM Kutta. Auftriebskräfte in strömenden flüssigkeiten. *Illustrierte Aeronautische Mitteilungen*, 6(133):133–135, 1902.

[11] DE Nakos and PD Sclavounos. On steady and unsteady ship wave patterns. *Journal of Fluid Mechanics*, 215:263–288, 1990.

[12] JN Newman. *Marine hydrodynamics*. The MIT press, 2018.